Vertically-Aligned Single-Crystal Nano-cone Arrays: Controlled Fabrication and Enhanced Field Emission

Jinglai Duan[1,2], Dang Yuan Lei[2*], Fei Chen[2], Shu Ping Lau[2], William I. Milne[3], Christina Trautmann[4], Jie Liu[1*]

[1] Materials Research Center, Institute of Modern Physics, Chinese Academy of Sciences, Lanzhou 730000, P. R. China

[2] Department of Applied Physics, The Hong Kong Polytechnic University, Hong Kong, China

[3] Department of Engineering, Electrical Engineering Division, University of Cambridge, 9 JJ Thomson Avenue, CB3 0FA , Cambridge , United Kingdom

[4] GSI Helmholtz Centre for Heavy Ion Research, 64291 Darmstadt, Germany

Abstract

Metal nanostructures with conical shape, vertical alignment, large aspect ratio, controlled cone angle, and single-crystal structure are ideal candidates for enhancing field electron emission efficiency with additional merits such as good mechanical and thermal stability. However, fabrication of such nanostructures possessing all these features still remains challenging. Here, we report on the controlled fabrication of large area, vertically aligned, and mechanically self-supported single-crystal Cu nano-cones with controlled cone angle and enhanced field emission. The Cu nano-cones were fabricated by ion track templates in combination with electrochemical deposition, and their cone angle is controlled in the range from 0.3° to 6.2° by asymmetrically selective etching of the ion tracks. The field emission measurements show that the turn-on electric field of the Cu nano-cone field emitters can be as low as 1.9 V/μm at current density of 10 μA/cm^2 and the maximum field enhancement factor can be as large as 6068, indicating that the Cu nano-cones are promising candidates for field emission applications.

Keywords: Nano-cone; Ion Track Template; Field Emission; Turn-on Field; Enhancement Factor

Introduction

Field emission, also known as field electron emission, is a fundamental physical phenomenon associate with quantum tunneling, in which electrons below or close to the Fermi level escape from the surface of materials by tunneling through surface potential barrier lowered with the aid of an external electric field [murphy56]. The field emission phenomenon has attracted growing research attention because it has important applications such as in high-power vacuum electronic devices,

microwave-generation devices, flat panel displays, vacuum microelectronic devices and nanoelectronic devices involved in the fields of consumer goods, military technology, and also space technology [milne04, xu05, zhai11]. These applications usually require field emitters having, some or all of the following characteristics: low turn-on field, high current density, long-term emission stability, miniaturized size, large area, and so on. To achieve a low turn-on field and a high current density which are the two most important parameters for all field emitters, the field emission materials should preferably have a low work function and be nanostructured with needle-like shapes because nanostructuring can give rise to significant field enhancement at the needle tips [xu05, zhai11]. The field enhancement factor β is directly proportional to tip height and inversely proportional to tip radius [xu05]. Apparently, it is important to make the needle tips as sharp as possible in order to reduce the applied external field required for turning on the emission [xu05, zhang14, zhai11, xu13].

The aforementioned fabrication guideline has strongly motivated the development of novel geometrically-sharp nanostructures for enhanced field emission. To date, several metal, semiconductor and carbon nanostructures have been developed in an attempt to achieve better field emission performance, including Ge and Cu nano-wires [li08, kim08], PrB_6 nano-rods [zhang08], WS_2 nano-tubes [viskadoros14], ZnO nano-walls [hong09], graphene nanoedges [Jiang13], boron nano-cones [li10], and many others [wang08, ye12, hallam14, chang09, xu06, xiao08]. Among these nanostructures, nano-cones have shown unique advantages, including good mechanical stability, large aspect ratio, low turn-on field, high emission current density, and large field-enhancement factor. Excellent examples are well demonstrated by wide band-gap semiconducting ZnO [zhang14, zeng09] and metallic nickel [joo06] nanostructures. In the past decade, several fabrication methods have been proposed to fabricate nano-cones, including ion-beam sputtering [shang02], reactive ion etching [zhang03], plasma etching [wang06], nanotransfer printing [kim081], chemical vapor deposition [wang07], template method [serbun12], wet chemical method [wang13], and electrochemical deposition [zhang14]. Although these various methods of fabrication have shown significant advantages in preparation of conical field emitters, the issues associated with relatively low height (shorter than 5 μm) [wang13], random or partially vertical alignment [xu13, wang13], field screening due to high density and large cone angle [zhang03, xu13, zhang13], large tip diameter [serbun12], and large height scattering [wang06], still

remain unsolved.

In this work, using copper as an example, vertically aligned single-crystal nano-cones with large and uniform height and controlled cone angle and areal density were prepared using a home-made ion track template in combination with electrochemical deposition. Taking advantage of the conical pore template obtained by asymmetrical etching of ion tracks, the cone angle can be controllably varied from 0.3° to 6.2°, which is impossible to achieve with other methods. Field emission measurements have shown that such nano-cones exhibit a dramatically decreased turn-on field compared to other counterparts. This is enabled by the huge field enhancement at the nano-cone tips as predicted by finite element simulations.

Experimental

Cu nanocones were fabricated by an ion track template with conical pores in combination with electrochemical deposition. Firstly, polycarbonate (PC) foils (Makrofol N, Bayer Leverkusen) of 30 μm in thickness were irradiated with 9.5 MeV/u $^{209}Bi^{31+}$ ions and 11.4 MeV/u $^{238}U^{28+}$ ions at normal incidence at the Heavy Ion Research Facility at Lanzhou (HIRFL) and the UNILAC linear accelerator, respectively. The irradiation fluence was 8×10^5 ions/cm^2 for both accelerators. To obtain conical nanopores, an asymmetric etching method was employed to etch out the tracks of the ions. The etchants were composed of various volume ratios of 9 M NaOH and methanol. Subsequently, Cu nano-cones were electrochemically deposited at 50 °C by applying a constant voltage of 200 mV. The electrolyte consisted of 75 g/l $CuSO_4{\cdot}5H_2O$ and 30 g/l H_2SO_4. A thin sputtered Au layer reinforced by an electroplated Cu layer was used as cathode for the Cu deposition. After dissolving the host PC template by dichloromethane, the morphology of nanocones was analyzed by scanning electron microscopy (SEM, Philips XL30 and FEI Nova NanoSEM 450). After detaching the cones from the supporting substrate using an ultrasonic field, the microstructure of the cones was investigated by high resolution transmission electron microscopy (HRTEM, FEI Tecnai G2 F20 S-TWIN). The field emission characteristics of the nanocones were measured in a vacuum chamber with a base pressure below 1×10^{-5} Pa. The measurements were conducted on a standard parallel-plate-electrode configuration where a stainless-steel plate was used as the anode, and each sample was fixed onto a copper stage which served as the cathode. The distance between the nano-cone tip and the anode was 300 μm. The *I-V* (current-voltage) curves were recorded by a computer-

controlled measurement system.

Results and discussion

The main fabrication procedures employed are schematically illustrated in Figure 1. Briefly, a PC foil is irradiated with swift heavy ions to create ion tracks (step 1). This was followed by sputtering deposition of a thin gold layer onto one surface of the PC foil as a cathode for subsequent etching of ion tracks and electrochemical deposition (step 2). The ion tracks are selectively etched out by asymmetric etching (step 3) in order to create conical pores which are subsequently filled with Cu to form Cu nano-cones using electrochemical deposition (step 4). Finally, over deposition is carried out to form a planar film to support the nano-cones (step 5), and the template matrix is removed by dichloromethane, leaving vertically aligned nanocones standing on the Cu film. Clearly, this method has unique advantages and high flexibility in fabricating nano-cone arrays because some key parameters including material, cone height, cone angle, and areal density can be flexibly selected.

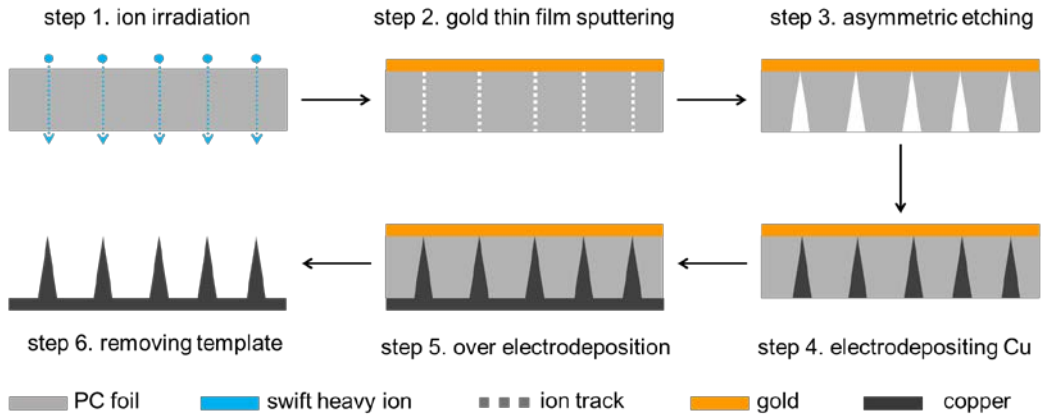

Figure 1. Schematic of the fabrication procedures of Cu nano-cones based on ion track template in combination with electrochemical deposition.

A representative SEM micrograph of a PC template is shown in Figure 2a. The conical pores are well separated and randomly distributed due to random hits of ions. The base diameter of pores is identical and the formation of conical pores is due to anisotropic etching of ion tracks. As is reported by Zhu et al [zhu04], two etch rates exist during the etching process, namely the track etching rate v_t (along track length) and the bulk etching rate v_b (perpendicular to track length), as

schematically shown in the inset of Figure 2a. The pore shape is determined by the ratio of the two rates. A cylindrical shape (often used to prepare nano-wires [liu06]) is obtained when v_t is much larger than v_b and a conical shape is obtained when v_t is comparable to v_b. During etching of the tracks, v_t is very sensitive to NaOH whereas v_b is relatively insensitive and thus a cylindrical shape is frequently formed. In this work, in order to enhance v_b, methanol is added to the NaOH etchant because methanol can dissolve bulk polycarbonate without significantly influencing v_t. After filling the conical pores with Cu by electrochemical deposition, the Cu nano-cone arrays were formed. A typical low-magnification SEM micrograph of arrays liberated from the template is displayed in Figure 2b. It can be seen that the nanocones are homogeneously distributed on the substrate over a large area, indicating that all pores were nearly fully filled. Note that unfilled pores would give rise to some small protrusions on the substrate (see step 4 in Figure 1). For comparison, an SEM image of a partially filled sample is shown in Figure S1 in the Supporting Information.

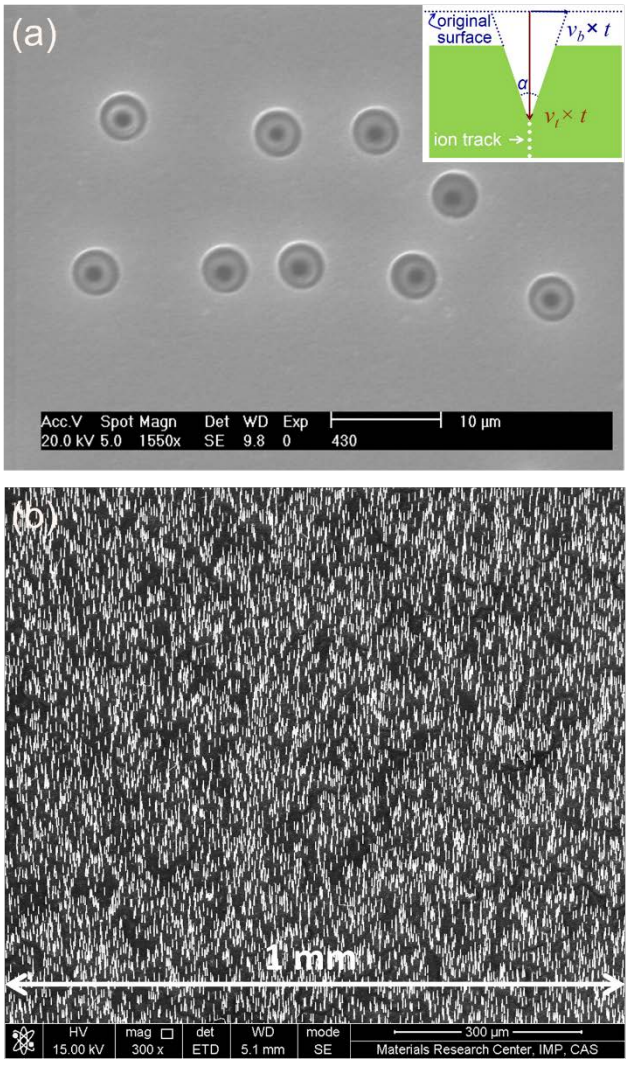

Figure 2. Typical SEM micrographs of a PC template with conical pores (a) and Cu nanocone arrays (b). The inset in (a) shows a schematic description of the track etching rate v_t and bulk etching rate v_b.

By changing the volume ratio of methanol to 9 M NaOH, we can tailor the cone angle of the conical pores and therefore the Cu nano-cones. Figure 3 shows the SEM images of the Cu nano-cones with different cone angles. All nano-cones show excellent conical shape and smooth, homogeneous contours along the their lengths. The tip diameter is about 50 nm and the length is nearly 30 μm which corresponds to the template thickness. By increasing the volume ratio of methanol to 9 M NaOH from 0 to 95%, the cone angle gradually increases from 0.3° to 6.2°.

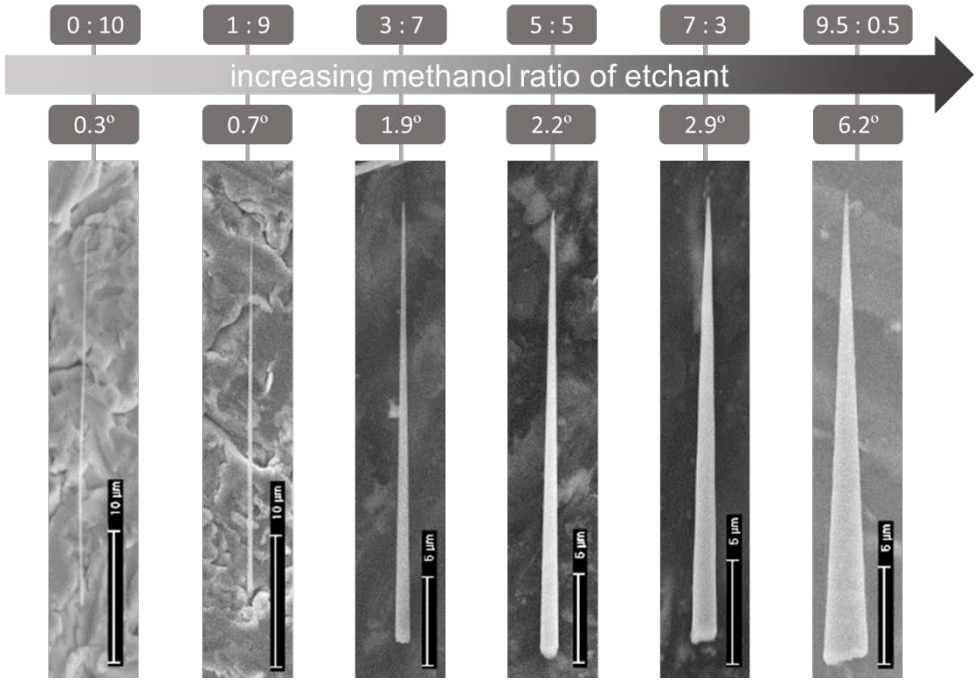

Figure 3. SEM micrographs of Cu nanocones with increased cone angle.

Good mechanical robustness is essential for enhanced and stable field emission. Therefore, mechanically self-supporting nano-cones are required for optimum emission performance. Figure 4 displays SEM images of nano-cone arrays with different cone angles. For a cone angle of 0.3° (Figure 4a), the nano-cones show very weak mechanical strength as previously observed for nano-wires [Duan08]. In Figure 4a, a large part of nano-cones collapse, aggregate, and support each other due to the small sizes both at the cone tip and the base. The mechanism of nano-cone

aggregation was proposed in our previous work [Duan08]. In addition to the aggregated cones, the others completely fall down. Such a geometrical configuration would limit the field emission due to increased tip size, reduced height, and smaller number of emitters. When the cone angle reaches 1.9° (Figure 4b), the majority of the nano-cones are well separated and vertically aligned. More cones are vertically standing and less cones fall down when the cone angle further increases to 2.6° (Figure 4c). We can see that at a cone angle 6.2° (Figure 4d) very few cones fall down, showing the best mechanical robustness.

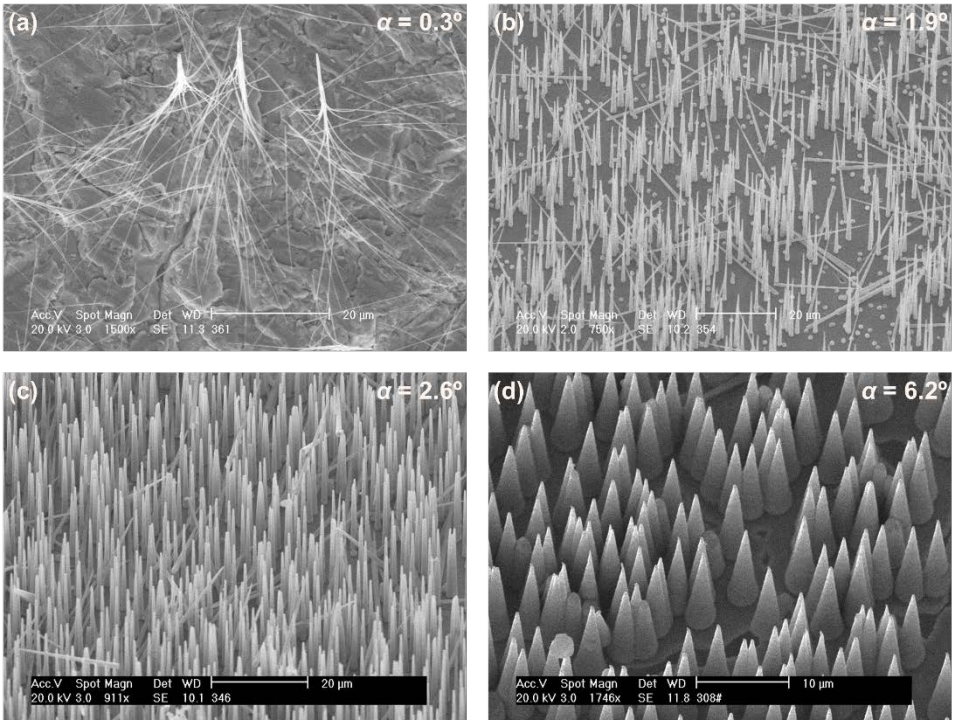

Figure 4. Representative SEM images of Cu nano-cone arrays with cone angles of 0.3° (a), 1.9° (b), 2.6° (c), and 6.2° (d).

The TEM images shown in Figure 5 reveal that the nano-cones have a perfect conical shape and are extremely straight despite a sharp decrease in the cone diameter at the proximity of the nano-cone apex. It is worthwhile pointing out that an ultrasonic field was used during sample preparation for TEM characterization, further corroborating the ultra-strong mechanical strength of the fabricated structures. In addition to the conical shape, single-crystal structures could be another important feature which is beneficial to improve mechanical strength because of reduced defects including voids, grain boundaries, and dislocations. The HRTEM images shown in the insets of Figure 5a clearly demonstrate that the nano-cone has a single-crystal structure, from the tip (the

upper left inset) to the middle of the cone (the lower right inset). Over several micrometers along the cone's length, no grain boundaries are observed. Note that, as a key parameter of the nano-cone structure, the apex diameter is extremely small and reaches 6 nm. It is worth mentioning that there exists two tip shapes, i.e. rounded tip (Figure 5a) and flat tip (Figure 5b).

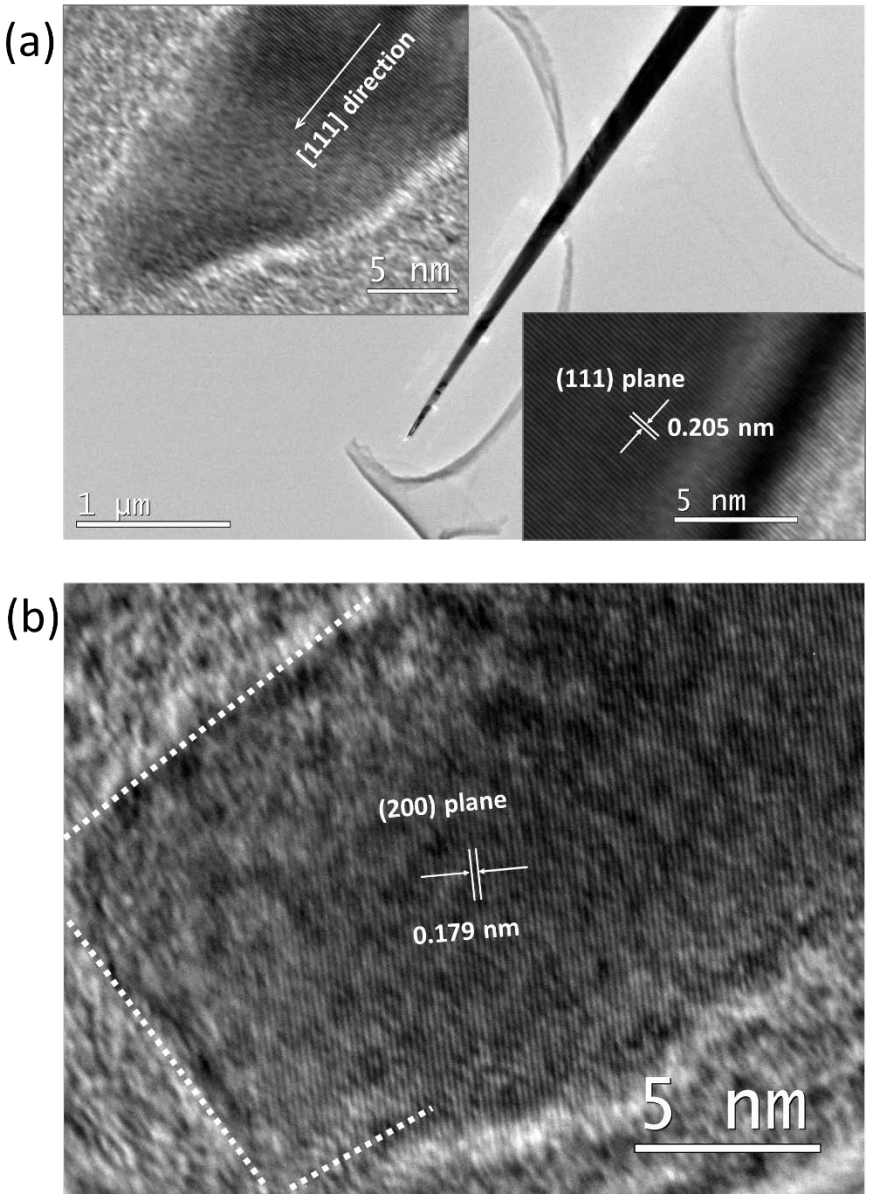

Figure 5. Representative TEM images of nanocones. (a) rounded tip, the insets are the HRTEM images of the cone tip (upper left) and from the middle of cone (lower right); (b) flat tip.

Taking advantage of their sharp tips, large heights, vertical alignment, and single-crystal structure, the present Cu nano-cones are expected to be excellent candidates for field electron emission and building blocks for electronic devices. To assess this, the current-voltage (*I-V*)

characteristics of the Cu nano-cones with cone angle of 6.2° and 2.9° were measured, respectively. For comparison, the field emission properties of a Cu nano-wire arrays of 75 nm in diameter, 2 μm in length, and 5×10^8 cm^{-2} in areal density were also measured. The SEM image of the nano-wires can be seen in the supporting information (Figure S2). Note that the nano-wires were electrochemically deposited at 100 mV at 50 °C and they possess single crystal structure as reported in our previous work [duan10]. The *I-V* curves of macroscopic applied field *E* versus emission current density *J* of the aforementioned three samples are presented in Figure 6a-c. As generally adopted [xu05, chang09], the turn-on field is defined as the field at which the current density reaches 10 $\mu A/cm^2$. As seen from Figure 6d, both nano-cone samples show significantly lower turn-on fields than the nano-wires. In particular, the Cu nano-cone sample with cone angle of 2.9° shows the best field emission properties with the lowest turn-on field of 1.9 V/μm (5.0 V/μm for the nano-cone sample with cone angle of 6.2° and 7.0 V/μm for the nano-wire sample). To the best of our knowledge, the turn-on field of 1.9 V/μm is a record low value compared with other reported values for other Cu nanostructures, e.g. 12.4 V/μm for nano-pillars, 4.6 V/μm for nano-wires, and 22 V/μm for nano-cones (Table 1). For a comprehensive comparison, Table 1 summarizes the key parameters of field emission, geometry, structure and material for various metallic nanostructures-based field emitters reported in previous literature and in this work. Furthermore, the turn-on field observed here is also much lower than those reported for nanostructures made of other materials as summarized in Refs. Xu05 and Cha12. All the three samples show similar maximum current densities of about 1.3 mA/cm^2. Taking into account the fact that the areal density of nano-cones is only 8×10^5 cm^{-2} which is nearly three orders of magnitude smaller than that of the nano-wires (5×10^8 cm^{-2}), the average emission current per nano-cone emitter is thus three orders of magnitude larger than that per nano-wire emitter, illustrating significantly enhanced field emission properties of single nano-cone emitters. It is worthwhile pointing out that the emission current measured in our nanocone sample is relatively stable over a whole measurement period of four hours at an intermediate vacuum degree of 1×10^{-5} Pa (see Figure S3 in the Supporting Information).

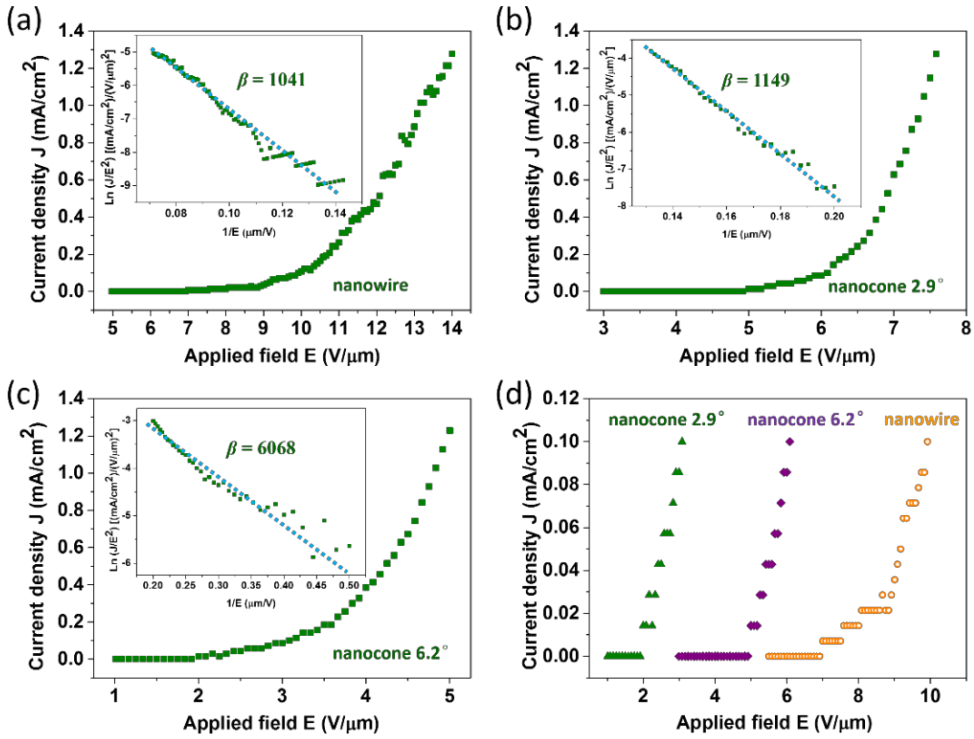

Figure 6. Field emission *J-E* curves for Cu nanowires (a), and nanocones with cone angle of 6.2° (b) and 2.9° (c), the insets are corresponding F-N plots. The turn-on fields of nanocones and nanowires are shown in (d). Labels are not right for (b) and (c).

For quantitative analysis, the Fowler-Nordheim (F-N) theory is usually employed to describe the field emission characteristics of materials and is expressed as [fowler28, banerjee04]

$$J = A_E \frac{\beta^2 E^2}{\emptyset} exp\left(\frac{-B_E \emptyset^{\frac{3}{2}}}{\beta E}\right) \quad (1)$$

or in a transformed form

$$ln\left(\frac{J}{E^2}\right) = ln\left(\frac{A_E \beta^2}{\emptyset}\right) - \frac{B_E \emptyset^{\frac{3}{2}}}{\beta E} \quad (2)$$

where A_E = 1.54 × 10^{-6} A eV V^{-2}, B_E = 6.83 × 10^3 $eV^{-3/2}\mu m^{-1}$, J is the current density, β is the field enhancement factor, E is the applied field, and ϕ is the work function of the emitter material. We can see from Eq. 2 that $\ln(J/E^2)$ is linearly proportional to $1/E$ with a slope of $-B_E\phi^{3/2}/\beta$. In other words, the field enhancement factor β can be deduced from the slope of F-N plot. In our calculation, the work function ϕ for copper is taken as 4.46 eV [kim08]. In Figures 6a-c, the insets are the corresponding F-N plots. The linear relationship of $\ln(J/E^2)$ versus $1/E$ of each sample implies that the electron emission from Cu nano-wires and nano-cones follow the F-N behavior, i.e. a process of tunneling of electrons through a potential barrier. The calculated field enhancement factors are

also shown in the insets. It is clearly seen that the nano-cone sample with cone angle of 2.9° possesses the largest field enhancement factor of 6068 (1149 for the nano-cone sample with cone angle of 6.2° and 1041 for the nano-wire sample), thereby leading to the lowest turn-on field.

Table 1. Key parameters of field emission, geometry, structure, and material for various metallic nanostructure-based field emitters reported in previous literature and this work.

Structure	Material	Turn-on field @ 10 μA/cm² [V/μm]	Field enhancement factor (β)	Alignment	Crystallinity	Effective height [μm]	Ref.
nanowire	Cu	4.6 at emission starts	443	partly	twinned crystal	~10.5	[kim08]
nanowire	Cu	~4.3-10	380-800	vertically	-	8-18	Maurer06
nanopillar	Cu	12.4	713	partly	single crystal	~7	[Chang09]
nanowire	Ni	4.0	1300	randomly	single crystal	-	[Joo06]
nanothorn	W	6.2	1578	randomly	single crystal	-	[baek06]
nanowire	Au	4.0 at 1 nA	Max. 630	partly, vertically	-	7-28	[navitski09]
nanowire	Ag	5.7 at emission starts	960	partly	polycrystal	10	[cha12]
nanowire	Co	12.0	211	vertically	-	2.1	[vila04]
nanowire	Ge	7.6 at 1μA/cm²	462	vertically	single crystal	-	[li08]
nanowire	Mo	2.2	4400	partly	single crystal	~3.1	[zhou03]
whisker	W	4.0	1904	partly	single crystal	20	[wang09]
nanopillar	Cu	12.4	713	partly	single crystal	~7	[Chang09]
nanocone	Cu	22-52	84-237	vertical	-	~28	[serbun12]
nanocone	Ni	5-6.7	1500-2000	vertically	single crystal	0.3-1.2	[hang10]
nanocone	Ni	4.1	3720	partly	single crystal	0.4	[wang13]
nanocone	Au	3.3 at 15 μA/cm²	2683	vertically	-	0.27	[kim081]
nanocone	AlN	4.2	1740	partly	single crystal	2	[liu09]
nanotaper	ZnO	9.3-11.3	226-304	partly	single crystal	2	[zhang14]
nanowire	Cu	7.0	1041	vertically	single crystal	2	this work
nanocone (6.2°)	Cu	5.0	1149	vertically	single crystal	28	this work
nanocone (2.9°)	Cu	1.9	6068	vertically	single crystal	28	this work

The maximized field emission enhancement of the nano-cones with cone angle of 2.9° can be attributed to their large height, sharp tip, vertical alignment, spatial separation, suppressed field shielding effects (due to intermediate cone angle), and single-crystal structure. The field emission enhancement is related to the aspect ratio of the emitters, i.e. the ratio of the nano-cone height and curvature radius at the apex [xu05, zhang13]. Apparently, a combination of large height and small radius would give rise to dramatic enhancement. In this work, the height of nano-cones is 28 μm and the minimum curvature radius at the rounded tip, as shown in the inset of Figure 5a, is smaller than 3 nm. Thus, the aspect ratio of nano-cones is greater than 9000, which generates huge field enhancement around the tip as demonstrated by the simulated electric field distribution

(Figure 7b). Furthermore, for the flat tip shown in Figure 5b, there exists a strong field enhancement around the circular edge, as evidenced by the numerical simulation shown in Figure 7c. Both types of the sharpness features are beneficial to the local field enhancement. Secondly, vertical alignment should be another critical factor that induces pronounced field enhancement. It has been widely observed that random alignment of metal nanostructures diminishes the effective height of the emitters and induces field shielding over neighboring emitters. Thirdly, spatial separation of the emitters is also responsible for field enhancement because close-packed arrays screen the applied field effectively [milne04]. Fourthly, an intermediate cone angle represents a balance between field emission enhancement and mechanical and thermal stability [milne04, utsumi91]. Finally, a single-crystal structure that is free of grain boundaries is an additional advantage for field emission enhancement because scattering of electrons and phonons at the grain boundaries can significantly decrease the electrical and thermal conductivity of the material.

To further understand the enhanced field emission of nano-cones, finite element simulations have been performed to calculate the electrostatic field strength as function of nano-cone tip shape and dimension by using the COMSOL Multiphysics software. The validation of the simulations was firstly verified by a simple model of a “hemisphere on a plane” (details are presented in the Supporting Information). In the simulations, the distance between the anode and the nanocone tip is 300 μm and the voltage applied over the distance is 1500 V, corresponding to a macroscopic applied field of 5 V/μm. Figures 7a and 7b show the electric field profile for two nano-cones with (a) a rounded tip and (b) a flat tip, and their tip diameter, base diameter, and nano-cone height are set to be 6 nm, 1.47 μm, and 28 μm, respectively. It can be clearly seen that both structures show significant field enhancement around the tip region and that the enhanced field tends to localize at the sharpest site (top of the rounded tip and edge of the flat tip), consistent with the field emission mechanism. To estimate the effect of tip diameter *d*, the field strength versus tip diameter is plotted in Figure 7c for both types of nano-cones, where the field strength increases dramatically with decreasing the tip diameter, consistent with our experimental observations, and the absolute field strength for the flat-tip nano-cone is slightly larger than the rounded-tip one. In addition, both curves can be perfectly fitted by the formula

$$E_{\mathrm{sim}} = \frac{a}{d^b} \tag{3}$$

where E_{sim} is the simulated field strength, and *a* and *b* are size-dependent constants. This formula implies that the field strength can be further increased by sharpening the nano-cone tip. In the experiments, nanometer- and even subnanometer-level sharp tips could be achieved by post-treatment of the as-grown nano-cones such as field-directed sputtering etching [schmucker12]. Therefore, a lower turn-on field and larger field enhancement factor would be expected, which we hope to investigate in follow-up work.

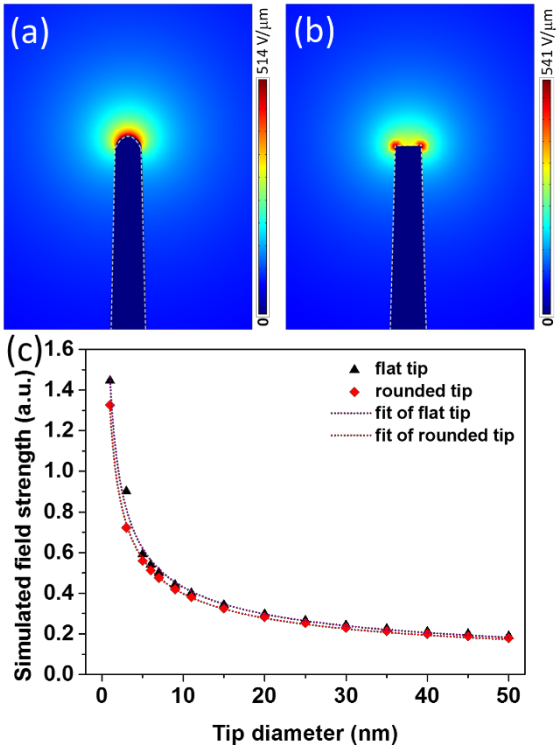

Figure 7. Simulated electric field profile for a single two-dimensional nano-cone with a rounded tip (a) or a flat tip (b). The white dashed line outlines the geometry of the nano-cone. (c) Simulated field strength versus tip diameter (black triangles for flat tip, red diamonds for rounded tip). The dashed lines are the fit to the simulated results using the formula (3). For the rounded (flat) tip, the fitting coefficients *a* and *b* are determined to be 1314.3 and 0.51863 (1462.1 and 0.53118).

Conclusion

In summary, we have shown that vertically aligned and mechanically self-supported single-crystal Cu nano-cone arrays can be fabricated by using ion track templates in combination with electrochemical deposition. The Cu nano-cones exhibit an aspect ratio up to 9000 and a wide range of cone angle from 0.3° to 6.2° which can be controlled the asymmetric etching process of the ion

track template. Benefiting from these unique geometrical and structural features, the Cu nano-cones with cone angle of 2.9° show dramatically enhanced field emission properties where the turn-on field is as low as 1.9 V/μm and the field enhancement factor is up to 6068. The results suggest that the Cu nano-cones made with ion track templates may be promising candidates for field electron emission applications. Due to the flexibility of the fabrication strategy, the method could be extended straightforwardly to prepare other materials based nano-cone structures including metals (Au, Ag, Pt etc.), semiconductors (e.g. CdS), and polymers (e.g. polypyrrole).

Acknowledgments

We thank the members of the Materials Research Department at the GSI Helmholtz-Zentrum (Darmstadt, Germany) for preparation and irradiation of some polycarbonate foils. The financial supports from the National Natural Science Foundation of China (Grant Nos.: 11175221, 11304261, 11375241, and 11179003) and the Hong Kong Research Grants Council (ECS Grant no. 509513) and the West Light Foundation of the Chinese Academy of Sciences are acknowledged. JLD thanks Dr. Th. W. Cornelius, Dr. H. J. Yao, and Dr. D. Mo for their valuable discussions.

Reference

[baek06] Yunho Baek, Yoonho Song, Kijung Yong, A Novel Heteronanostructure System: Hierarchical W Nanothorn Arrays on WO_3 Nanowhiskers, Advanced Materials 18(2006)3105-3110.

[banerjee04] Debasish Banerjee, Sung Ho Jo, Zhi Feng Ren, Enhanced Field Emission of ZnO Nanowires, Advanced Materials 16(2004)2028-2032.

[cha12] Indrani Chakraborty, Pushan Ayyub, Controlled clustering in metal nanorod arrays leads to strongly enhanced field emission characteristics, Nanotechnology 23(2012)015704 (7pp)

[chang09] I-Chun Chang, Ting-Kai Huang, Huang-Kai Lin, Yu-Feng Tzeng, Chih-Wei Peng, Fu-Ming Pan, Chi-Young Lee, Hsin-Tien Chiu, Growth of Pagoda-Topped Tetragonal Copper Nanopillar Arrays, ACS Applied Materials & Interfaces 1(2009)1375-1378.

[duan10] Jinglai Duan, Jie Liu, Dan Mo, Huijun Yao, Khan Maaz, Yonghui Chen, Youmei Sun, Mingdong Hou, Xiaohua Qu, Ling Zhang, Yanfeng Chen, Controlled crystallinity and crystallographic orientation of Cu nanowires fabricated in ion-track templates, Nanotechnology 21(2010)365605 (8pp).

[fowler28] R. H. Fowler, L. Nordheim, Electron Emission in Intense Electric Fields, Proceedings of the Royal Society of London. Series A 119(1928)173-181.

[hallam14] Toby Hallam, Matthew T. Cole, William I. Milne, Georg S. Duesberg, Field Emission Characteristics of Contact Printed Graphene Fins, Small 10(2014)95-99.

[hang10] Tao Hang, Huiqin Ling, Anmin Hu, Ming Li, Growth Mechanism and Field Emission Properties of Nickel Nanocones Array Fabricated by One-Step Electrodeposition, Journal of The Electrochemical Society 157(2010)D624-D627.

[hong09] Young Joon Hong, Hye Seong Jung, Jinkyoung Yoo, Yong-Jin Kim, Chul-Ho Lee, Miyoung Kim, Gyu-Chul Yi, Shape-Controlled Nanoarchitectures Using Nanowalls, Advanced Materials 21(2009)222-226.

[jiang13] Lili Jiang, Tianzhong Yang, Fei Liu, Jing Dong, Zhaohui Yao, Chengmin Shen, Shaozhi Deng, Ningsheng Xu, Yunqi Liu, Hongjun Gao, Advanced Materials 25(2013)250-255.

[joo06] Jinsoo Joo, Sun Jeong Lee, Dong Hyuk Park, Young Soo Kim, Yeonhee Lee, Cheol Jin Lee, Seong-Rae Lee, Field emission characteristics of electrochemically synthesized nickel nanowires with oxygen plasma post-treatment, Nanotechnology 17(2006)3506-3511.

[kim08] Changwook Kim, Wenhua Gu, Martha Briceno, Ian M. Robertson, Hyungsoo Choi, Kyekyoon (Kevin) Kim, Copper Nanowires with a Five-Twinned Structure Grown by Chemical Vapor Deposition, Advanced Materials 20(2008)1859-1863.

[kim081] Tae-il Kim, Ju-hyung Kim, Sang Jun Son, Soon-min Seo, Gold nanocones fabricated by nanotransfer printing and their application for field emission, Nanotechnology 19(2008)295302(4pp).

[li08] Liang Li, Xiaosheng Fang, Han Guan Chew, Fei Zheng, Tze Haw Liew, Xijin Xu, Yunxia Zhang, Shusheng Pan, Guanglai Li, Lide Zhang, Crystallinity-Controlled Germanium Nanowire Arrays: Potential Field Emitters, Advanced Materials 18(2008)1080-1088.

[li10] Chen Li, Yuan Tian, Chao Hui, Jifa Tian, Lihong Bao, Chengmin Shen, Hong-Jun Gao, Field emission properties of patterned boron nanocones, Nanotechnology 21(2010)325705 (5pp).

[liu06] J. Liu, J. L. Duan, M. E. Toimil-Molares, S. Karim, T. W. Cornelius, D. Dobrev, H. J. Yao, M. D. Hou, D. Mo, Z. G. Wang, R. Neumann, Electrochemical fabrication of single-crystalline and polycrystalline Au nanowires: the influence of deposition parameters, Nanotechnology 17(2006)1922-1926.

[liu09] Fei Liu, Zan-Jia Su, Wei-Jie Liang, Fu-Yao Mo, Li Li, Shao-Zhi Deng, Jun Chen, Ning-Sheng Xu, Controlled growth and field emission of vertically aligned AlN nanostructures with different morphologies, Chinese Physics B 18(2009)2016-2023.

[maurer06] Florian Maurer, Arti Dangwal, Dmitry Lysenkov, Gunter Muller, Maria Eugenia Toimil-Molares, Christina Trautmann, Joachim Brotz, Hartmut Fuess, Field emission of copper nanowires grown in polymer ion-track membranes, Nuclear Instruments and Methods in Physics Research B 245 (2006) 337-341.

[milne04] W. I. Milne, K. B. K. Teo, G. A. J. Amaratunga, P. Legagneux, L. Gangloff, J.-P. Schnell, V. Semet, V. Thien Binh, O. Groening, Carbon nanotubes as field emission sources, Journal of Materials Chemistry 14(2004)933-943.

[murphy56] E. L. Murphy, R. H. Good, Jr. Thermionic Emission, Field Emission, and the Transition Region, Phys. Rev. 102(1956)1464-1473.

[navitski09] A. Navitski, G. Muller, V. Sakharuk, T. W. Cornelius, C. Trautmann, S. Karim, Efficient field emission from structured gold nanowire cathodes, The European Physical Journal Applied Physics 48(2009)30502 (7pp)

[serbun12] P. Serbun, F. Jordan, A. Navitski, G. Müller, I. Alber, M.E. Toimil-Molares, and C. Trautmann, Copper nanocones grown in polymer ion-track membranes as field

emitters, Eur. Phys. J. Appl. Phys. 58(2012)10402.

[shang02] Nai Gui Shang, Fan Yu Meng, Frederick C. K. Au, Quan Li, Chun Sing Lee, Igor Bello, Shuit Tong Lee, Fabrication and Field Emission of High-Density Silicon Cone Arrays, Advanced Materials 14(2002)1308.

[utsumi91] Takao Utsumi, Vacuum Microelectronics: What's New and Exciting, IEEE Transaction on Electron Devices, 38(1991)2276-2283.

[vila04] Laurent Vila, Pascal Vincent, Laurence Dauginet-De Pra, Gilles Pirio, Eric Minoux, Laurent Gangloff, Sophie Demoustier-Champagne, Nicolas Sarazin, Etienne Ferain, Roger Legras, Luc Piraux, Pierre Legagneux, Growth and Field-Emission Properties of Vertically Aligned Cobalt Nanowire Arrays, Nano Letters 4(2004)521-524.

[viskadoros14] G. Viskadouros, A. Zak, M. Stylianakis, E. Kymakis, R. Tenne, E. Stratakis, Enhanced Field Emission of WS_2 Nanotubes, Small 10(2014)2398-2403.

[wang06] Q. Wang, Z. L. Wang, J. J. Li, Y. Huang, Y. L. Li, C. Z. Gu, Z. Cui, Field electron emission from individual diamond cone formed by plasma etching, Applied Physics Letters 89(2006)063105.

[wang07] Xingjun Wang, Jifa Tian, Tianzhong Yang, Lihong Bao, Chao Hui, Fei Liu, Chengmin Shen, Changzhi Gu, Ningsheng Xu, Hongjun Gao, Single Crystalline Boron Nanocones: Electric Transport and Field Emission Properties, Advanced Materials 19(2007)4480-4485.

[wang08] Ming-Sheng Wang, Qing Chen, Lian-Mao Peng, Field-Emission Characteristics of Individual Carbon Nanotubes with a Conical Tip: The Validity of the Fowler–Nordheim Theory and Maximum Emission Current, Small 4(2008)1907-1912.

[wang09] Shiliang Wang, Yuehui He, Xiaosheng Fang, Jin Zou, Yong Wang, Han Huang, Pedro M. F. J. Costa, Min Song, Baiyun Huang, Chain T. Liu, Peter K. Liaw, Yoshio Bando, Dmitri Golberg, Structure and Field-Emission Properties of Sub-Micrometer-Sized Tungsten-Whisker Arrays Fabricated by Vapor Deposition, Advanced Materials 21(2009)2387-2392.

[wang13] Jian Wang, Liangming Wei, Liying Zhang, Jing Zhang, Hao Wei, Chuanhai Jiang, Yafei Zhang, Controlled growth of nickel nanocrystal arrays and their field electron emission performance enhancement via removing adsorbed gas molecules, CrystEngComm 15(2013)1296-1306.

[xiao08] Jing Xiao, Xianxiang Zhang, Gengmin Zhang, Field emission from zinc oxide nanotowers: the role of the top morphology, Nanotechnology 19(2008)295706 (6pp)

[xu05] N. S. Xu, S. E. Huq, Novel cold cathode materials and applications, Materials Science and Engineering R 48(2005)47-189.

[xu06] Feng Xu, Ke Yu, Guodong Li, Qiong Li and Ziqiang Zhu, Synthesis and field emission of four kinds of ZnO nanostructures: nanosleeve-fishes, radial nanowire arrays, nanocombs and nanoflowers, Nanotechnology 17(2006)2855-2859.

[xu13] Junqi Xu, Guanghua Hou, Huiqiao Li, Tianyou Zhai, Baoping Dong, Hailong Yan, Yanrui Wang, Benhai Yu, Yoshio Bando, Dmitri Golberg, Fabrication of vertically aligned single-crystalline lanthanum hexaboride nanowire arrays and investigation of their field emission, NPG Asia Materials 5(2013)e53.

[ye12] Dexian Ye, Sherif Moussa, Josephus D. Ferguson, Alison A. Baski, M. Samy El-Shall, Highly Efficient Electron Field Emission from Graphene Oxide Sheets Supported by Nickel

Nanotip Arrays, Nano Letters 12(2012)1265-1268.

[zeng09] Haibo Zeng, Xijin Xu, Yoshio Bando, Ujjal K. Gautam, Tianyou Zhai, Xiaosheng Fang, Baodan Liu, Dmitri Golberg, Template Deformation-Tailored ZnO Nanorod/Nanowire Arrays: Full Growth Control and Optimization of Field-Emission, Advanced Functional Materials 19(2009)3165-3172.

[zhang03] W. J. Zhang, Y. Wu, W. K. Wong, X. M. Meng, C. Y. Chan, I .Bello, Y. Lifshitz, S. T. Lee, Structuring nanodiamond cone arrays for improved field emission, Applied Physics Letters 83(2003)3365-3367.

[zhang08] Qin Yuan Zhang, Jun Qi Xu, Yan Ming Zhao, Xiao Hong Ji, Shu Ping Lau, Fabrication of Large-Scale Single-Crystalline PrB_6 Nanorods and Their Temperature-Dependent Electron Field Emission, Advanced Functional Materials 19(2009) 742-747.

[zhang14] Zhuo Zhang, Guowen Meng, Qiang Wu, Zheng Hu, Jingkun Chen, Qiaoling Xu, Fei Zhou, Enhanced Cold Field Emission of Large-area Arrays of Vertically Aligned ZnO-nanotapers via Sharpening: Experiment and Theory, Scientific Reports, 4(2014)4676.

[zhou03] Jun Zhou, Ning-Sheng Xu, Shao-Zhi Deng, Jun Chen, Jun-Cong She, Zhong-Lin Wang, Large-Area Nanowire Arrays of Molybdenum and Molybdenum Oxides: Synthesis and Field Emission Properties, Advanced Materials 15(2003)1835-1840.

[zhu04] Z. Y. Zhu, J. L. Duan, Y. Maekawa, H. Koshikawa, M. Yoshida, Bulk and track etching of PET studied by spectrophotometer, Radiation Measurements 38(2004)255-261.

[zhai11] Tianyou Zhai, Liang Li, Ying Ma, Meiyong Liao, Xi Wang, Xiaosheng Fang, Jiannian Yao, Yoshio Bando, Dmitri Golberg, One-dimensional inorganic nanostructures: synthesis, field-emission and photodetection, Chem. Soc. Rev. 40(2011)2986-3004.

[duan08] Jing-Lai Duan, Jie Liu, Hui-Jun Yao, Dan Mo, Ming-Dong Hou, You-Mei Sun, Yan-Feng Chen, Ling Zhang, Controlled synthesis and diameter-dependent optical properties of Cu nanowire arrays, Materials Science and Engineering B 147 (2008) 57-62.

[schmucker12] S. W. Schmucker, N. Kumar, J. R. Abelson, S. R. Daly, G. S. Girolami, M. R. Bischof, D. L. Jaeger, R. F. Reidy, B. P. Gorman, J. Alexander, J. B. Ballard, J. N. Randall, J. W. Lyding, Field-directed sputter sharpening for tailored probe materials and atomic-scale lithography, Nature Communications 3(2012)935 (8pp).